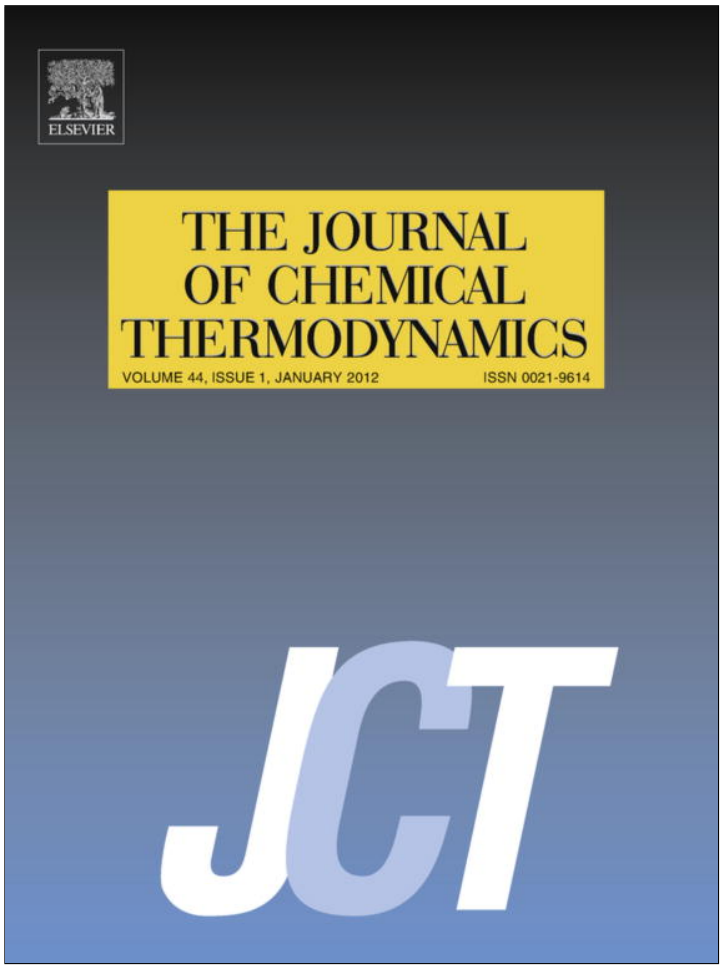

J. Chem. Thermodynamics 44 (2012) 97–101

Contents lists available at SciVerse ScienceDirect

J. Chem. Thermodynamics

journal homepage: www.elsevier.com/locate/jct

A corresponding states treatment of the liquid–vapor saturation line

K. Srinivasan [a,b], K.C. Ng [a], S. Velasco [c], J.A. White [c,d,*]

[a] Department of Mechanical Engineering, National University of Singapore, Singapore 117576, Singapore
[b] Department of Mechanical Engineering, University of Melbourne, Vic 3010, Australia
[c] Departamento de Física Aplicada, Universidad de Salamanca, 37008 Salamanca, Spain
[d] IUFFyM, Universidad de Salamanca, 37008 Salamanca, Spain

ARTICLE INFO

Article history:
Received 16 May 2011
Received in revised form 21 July 2011
Accepted 4 August 2011
Available online 11 August 2011

Keywords:
Corresponding states
Vapor pressure curve
Saturation properties
Srinivasan's points

ABSTRACT

In this work we analyze correlations for the maxima of products of some liquid–vapor saturation properties. These points define new characteristic properties of each fluid that are shown to exhibit linear correlations with the critical properties. We also demonstrate that some of these properties are well correlated with the acentric factor. An application is made to predict the properties of two new low global warming potential (GWP) refrigerants.

1. Introduction

The liquid–vapor phase transition continues to enthrall the science and engineering communities. Several features of scientific interest are being unraveled and saturation properties are also the first to be considered in the design of engineering systems such as vapor compression based refrigeration, heat pumping devices and Rankine cycle based power generating units. A number of interesting features have already been brought forth by several researchers [1–3]. Among them are the saturated liquid density [4], the enthalpy of vaporization [5–8], the vapor pressure curve [9–12], and the saturated liquid phase velocity of sound [13]. In addition, far reaching implications of the relation between the saturation pressure where the product of temperature and liquid density is the largest and the maximum in the peak nucleate boiling heat flux have also been appreciated [14]. The primary focus in most of these papers has been either fluids for refrigeration and heat pumping (because of the push to replace ozone depleting working fluids consequent to the ratification of the Montreal protocol by several countries) or proving the basic premise of some of the postulates with a few representative fluids. With a fresh impetus on newer fluids in the aftermath of global warming and emphasis on reduction of greenhouse gas emissions, urgency has arisen to revisit the whole gamut of fluids at our disposal and to assess the desirable thermodynamic properties of low global warming potential (GWP) fluids.

In this context, in 2002 Srinivasan [11] observed that the reduced temperature $T_r \equiv T/T_c$ (T_c is the critical temperature) and the reduced pressure $p_r \equiv p/p_c$ (p_c is the critical pressure) can be used to build the functions $\phi_{1r} \equiv T_r\,(1 - p_r)$ and $\phi_{2r} \equiv p_r(1 - T_r)$, which always exhibit a peak along the vapor pressure curve. Srinivasan also observed that the reduced temperatures T_{sp1r} and T_{sp2r}, at which ϕ_{1r} and ϕ_{2r}, respectively, attain the maximum, showed a linear correlation. Later on, Velasco *et al.* [15] covered 1214 fluids and established that the linear relation between the two Srinivasan's points generally holds good except at extreme cases. They also proposed a polynomial relation between the two points along the vapor pressure curve. Tian *et al.* [16] also report that the criterion of a maximum $p_r(1 - T_r)$ can be used to optimize the coefficients in cubic equations of state. These two points on the vapor pressure curve set the limits of operation of several practical thermodynamic cycles. The objective of this paper is to derive some generalized correlations related to several other saturation properties. They are the relation between the temperature at which the maximum in the product of saturation temperature and liquid density exists vs the critical temperature, and the temperature at which the saturated vapor enthalpy is a maximum [17].

The NIST Chemistry WebBook [18] database has been used in assessing various entities described in this paper because it is able to meet the current needs of scientific accuracy and industrial relevance. We have considered the 75 fluids available in this database. A list of these fluids together with their critical parameters and other quantities defined in this work is presented in tables S1 and S2 of

* Corresponding author at: Departamento de Física Aplicada, Universidad de Salamanca, 37008 Salamanca, Spain. Tel.: +34 923294436; fax: +34 923294584.
E-mail address: white@usal.es (J.A. White).

0021-9614/$ - see front matter © 2011 Elsevier Ltd. All rights reserved.
doi:10.1016/j.jct.2011.08.005

the supplementary data. It is expected that the present article would be of use in the first order estimate of properties of newer fluids being synthesized (such as hydrofluoro-olefins and hydrofluoroalkenes like R-1234yf) for meeting the exigencies of low global warming working fluid requirements. However, this paper does not address other issues of application such as toxicity and flammability that are seldom described from an analysis of saturation properties.

2. First formulation: salient points obtained from the coexistence curve

Srinivasan and Krishna Murthy [4] reported that all fluids have a maximum in the product $\psi \equiv T\rho_f$ of saturation temperature and liquid density, and that the reduced temperature at this point has a value around 0.82, which is weakly dependent on the complexity of the liquid molecule. As depicted in figure 1, we find that the temperature T^* where $\psi_{\max}$ occurs bears the following linear relationship with the critical temperature T_c:

$$T^*/\mathrm{K} = 0.8862 + 0.8109(T_c/\mathrm{K}). \tag{1}$$

This expression gives a better picture of the correlation between T^* and T_c than the observation of constancy of T^*/T_c.

In order to perform a more detailed analysis of the correlations we define the relative deviation Δ_r of a tabulated value f from the value obtained using the correlation as

$$\Delta_r \equiv 1 - \frac{f_{\text{correlation}}}{f_{\text{tabulated}}}. \tag{2}$$

The inset of figure 1 shows the percent relative deviation ($10^2\Delta_r$) of T^* for the fluids considered in this work. The average absolute relative deviation for all fluids is $\Delta_{\text{av}} = 0.61\%$. The maximum absolute relative deviation is obtained for Helium with a value $\Delta_{\max} = 12.22\%$. The average absolute relative deviation is defined as

$$\Delta_{\text{av}} \equiv \frac{1}{n}\sum_i^n |\Delta_{r,i}| = \frac{1}{n}\sum_i^n \left|1 - \frac{f_{\text{correlation},i}}{f_{\text{tabulated},i}}\right|, \tag{3}$$

while the maximum absolute relative deviation is

$$\Delta_{\max} \equiv \max|\Delta_{r,i}| = \max\left|1 - \frac{f_{\text{correlation},i}}{f_{\text{tabulated},i}}\right|. \tag{4}$$

We also have determined the coefficient of determination for this correlation, obtaining a value $R^2 = 0.9997$. We note that this coefficient is defined as

$$R^2 \equiv 1 - \frac{\sum_i^n (f_{\text{tabulated},i} - f_{\text{correlation},i})^2}{\sum_i^n (f_{\text{tabulated},i} - \bar{f}_{\text{tabulated}})^2}. \tag{5}$$

where

$$\bar{f}_{\text{tabulated}} \equiv \frac{1}{n}\sum_i^n f_{\text{tabulated},i} \tag{6}$$

is the average value of the tabulated data.

Srinivasan and Krishna Murthy [4] also proposed that the molecular diameter σ can be approximated as follows [4]

$$\sigma = \left(\frac{V_{fT^*}}{\sqrt{2}N}\right)^{1/3}, \tag{7}$$

where $V_{fT^*} = M/\rho_f^*$ is the molar volume (M is the molar mass) at T^* and N is the Avogadro number. In deriving this relation it is assumed that the Lennard-Jones 12-6 potential governs the molecular interactions.

A correlation involving σ can be found by representing this molecular length parameter as a function of the Lennard-Jones intermolecular separation at zero potential energy σ_c, which in terms of the critical molar volume V_c is given by [19]

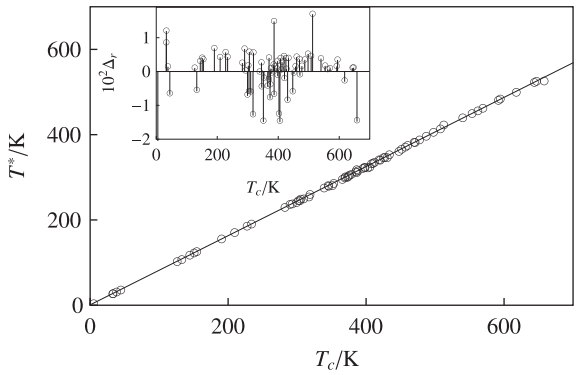

FIGURE 1. Temperature T^* where $\psi \equiv T\rho_f$ attains its maximum value *vs.* the critical temperature T_c. The symbols are the values obtained for the 75 fluids included in the NIST Chemistry WebBook [18] (see table S1 of the supplementary data). The solid line represents equation (1). The inset shows the percent relative deviations of T^*.

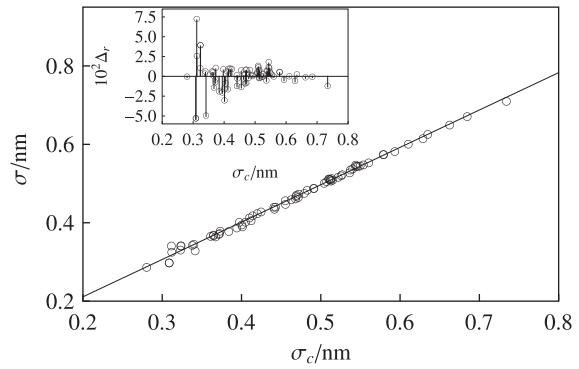

FIGURE 2. The molecular length parameter σ *vs.* the Lennard-Jones intermolecular separation at zero potential energy σ_c. The symbols are the values obtained for the 75 fluids included in the NIST Chemistry WebBook [18] (see table S1 of the supplementary data). The solid line represents equation (9). The inset shows the percent relative deviations of σ.

$$N\sigma_c^3 = 0.317V_c. \tag{8}$$

This is shown in figure 2, where we also plot the linear fit

$$\sigma/\mathrm{nm} = 0.02049 + 0.9530(\sigma_c/\mathrm{nm}), \tag{9}$$

with $R^2 = 0.9956$, $\Delta_{\text{av}} = 1.07\%$, and $\Delta_{\max} = 7.13\%$ for Helium.

This is equivalent to a plot of ρ_f^* *vs.* ρ_c and is shown in figure 3. It is evident that a good linear correlation exists:

$$\rho_f^*/(\mathrm{kg}\cdot\mathrm{m}^{-3}) = 18.216 + 2.209\rho_c/(\mathrm{kg}\cdot\mathrm{m}^{-3}), \tag{10}$$

with $R^2 = 0.9924$. We also obtain $\Delta_{\text{av}} = 5.217\%$, and $\Delta_{\max} = 47.59\%$ for Hydrogen.

At the point where $\psi = T\rho_f$ attains its maximum value one has

$$\alpha_\sigma \equiv -\frac{1}{\rho_f}\frac{\partial\rho_f}{\partial T}\bigg|_{T^*} = \frac{1}{T^*}, \tag{11}$$

where we note that α_σ cannot be construed to be the thermal expansion coefficient (α) because it is not obtained at constant pressure. Yet, the difference in temperatures between points where each of them is equal to the inverse of temperatures is not significantly different for most fluids.

3. Second formulation: maxima along the vapor pressure curve

As mentioned in the introduction, the existence of a maximum in $\phi_{1r} = T_r(1 - p_r)$ and $\phi_{2r} = p_r(1 - T_r)$ along the vapor pressure

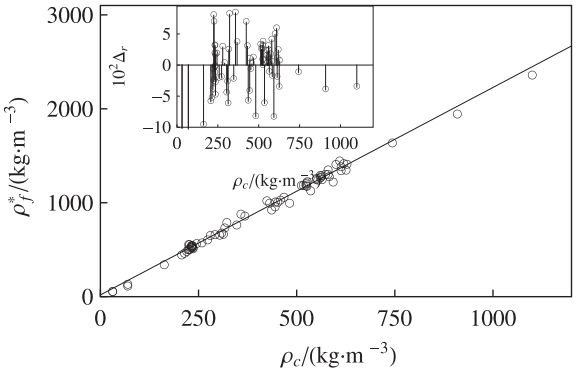

FIGURE 3. Correlation between densities at T_c and T^*. The symbols are the values obtained for the 75 fluids included in the NIST Chemistry WebBook [18] (see table S1 of the supplementary data). The solid line represents equation (10). The inset shows the percent relative deviations of ρ_f^*.

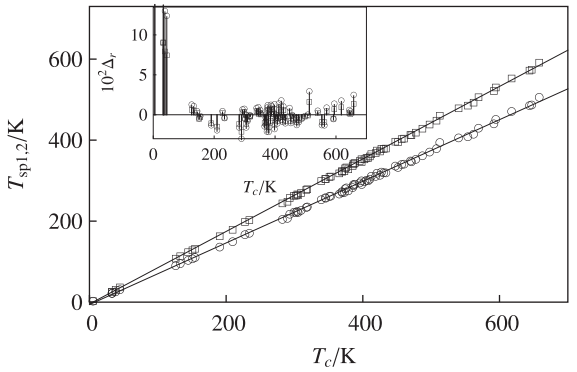

FIGURE 4. Temperatures T_{sp1} (where $T(p_c - p)$ is maximum) and T_{sp2} (where $p(T_c - T)$ is maximum) *vs.* the critical temperature T_c. The circles represent T_{sp1} and the squares are T_{sp2} for the 75 fluids included in the NIST Chemistry WebBook [18] (see table S1 of the supplementary data). The solid lines represent equations (12) and (13). The inset shows the percent relative deviations of T_{sp1} (○) and T_{sp2} (□).

curve has been brought out in recent years [11,15]. The reduced temperatures T_{sp1r} and T_{sp2r} at which these functions attain the maximum and the maximum values $\bar{\phi}_{sp1r}$ and $\bar{\phi}_{sp2r}$ themselves can be well correlated. We further observe (figure 4) that there are also linear correlations between the critical temperature T_c and the temperatures $T_{sp1} = T_{sp1r}T_c$ and $T_{sp2} = T_{sp2r}T_c$ at which those maxima occur. We obtain:

$$T_{sp1}/\mathrm{K} = 0.7609(T_c/\mathrm{K}) - 6.0155, \tag{12}$$

with $R^2 = 0.9989$, $\Delta_{av} = 3.78\%$, and $\Delta_{max} = 160.02\%$ for Helium.

$$T_{sp2}/\mathrm{K} = 0.8951(T_c/\mathrm{K}) - 4.5368, \tag{13}$$

with $R^2 = 0.9996$, $\Delta_{av} = 2.30\%$, and $\Delta_{max} = 97.26\%$ for Helium.

Analogously, $p_{sp1} \equiv p(T_{sp1}) = \bar{\phi}_{sp1r}p_c/(1 - T_{sp1r})$ and $p_{sp2} \equiv p(T_{sp2}) = (1 - \bar{\phi}_{sp2r}/T_{sp2r})p_c$ also hold similar linear relationships with p_c as shown in figure 5 and the correlations are given below:

$$p_{sp1}/\mathrm{MPa} = 0.09500(p_c/\mathrm{MPa}) + 0.03353, \tag{14}$$

with $R^2 = 0.9819$, $\Delta_{av} = 9.09\%$, and $\Delta_{max} = 37.05\%$ for Dodecane.

$$p_{sp2}/\mathrm{MPa} = 0.4032(p_c/\mathrm{MPa}) + 0.01567, \tag{15}$$

with $R^2 = 0.9998$, $\Delta_{av} = 1.03\%$, and $\Delta_{max} = 14.02\%$ for Helium.

Traditionally, the acentric factor ($\omega \equiv -\log_{10}(p_r) - 1$ at $T_r = 0.7$) has been used as a parameter characterizing the saturation vapor pressure. It is worthwhile examining its relation with the three maxima discussed above. Figure 6 shows a summary of the behavior. It is apparent that ω correlates very well with $T_{sp1r}(1 - p_{sp1r}) = \bar{\phi}_{sp1r}p_cT_c$

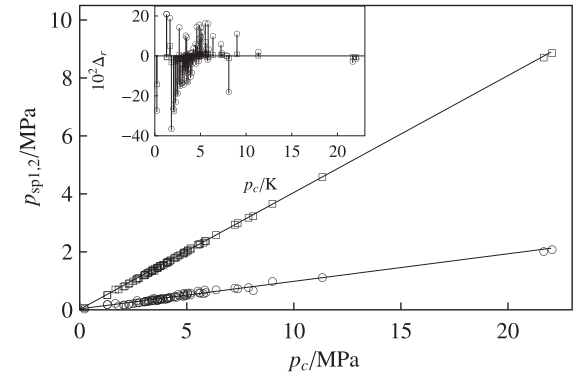

FIGURE 5. Pressures p_{sp1} (where $T(p_c - p)$ is maximum) and p_{sp2} (where $p(T_c - T)$ is maximum) *vs.* the critical pressure p_c. The circles represent p_{sp1} and the squares are p_{sp2} for the 75 fluids included in the NIST Chemistry WebBook [18] (see table S2 of the supplementary data). The solid lines represent equations (14) and (15). The inset shows the percent relative deviations of p_{sp1} (○) and p_{sp2} (□).

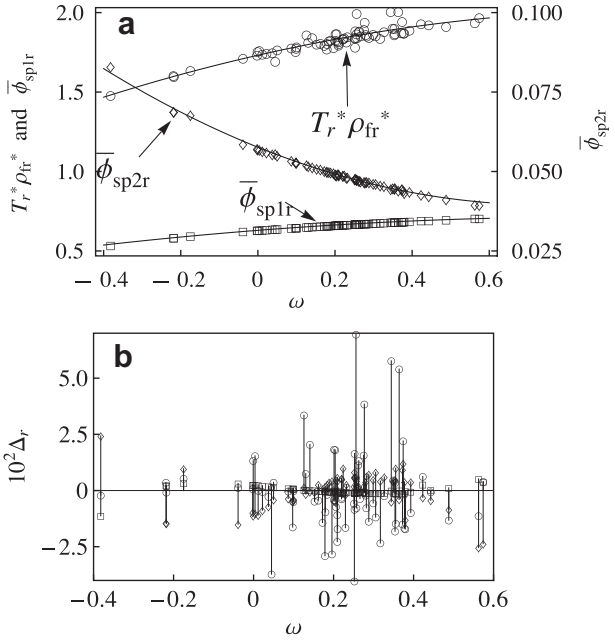

FIGURE 6. (a) Relationship between $\bar{\phi}_{sp1r} = T_{sp1r}(1 - p_{sp1r})$, $\bar{\phi}_{sp2r} = p_{sp2r}(1 - T_{sp2r})$ (right ordinate), $T_r^*\rho_{fr}^*$ and the acentric factor ω. The symbols represent our results for the 75 fluids included in the NIST Chemistry WebBook [18] (see table S2 of the supplementary data). The solid lines are equations (16)–(18) and (b) percent relative deviations of $\bar{\phi}_{sp1r}$ (□), $\bar{\phi}_{sp1r}$ (◇), and $T_r^*\rho_{fr}^*$ (○).

and $p_{sp2r}(1 - T_{sp2r}) = \bar{\phi}_{sp2r}p_cT_c$ and reasonably with $\psi_{max} = T_r^*\rho_{fr}^*$. Evidently, these relations are not linear. The noise in the correlation in the last one can be ascribed in most cases to equations of state that are not accurate enough whereas in other cases it rises due to compounding of molecular complexities that affect T_r^* and ρ_f^*. We obtain the following quadratic correlations:

$$T_{sp1r}(1 - p_{sp1r}) = -0.1055\omega^2 + 0.1892\omega + 0.6297, \tag{16}$$

with $R^2 = 0.9981$, $\Delta_{av} = 1.28\%$, and $\Delta_{max} = 6.95\%$ for Ammonia.

$$p_{sp2r}(1 - T_{sp2r}) = 0.03274\omega^2 - 0.04874\omega + 0.05763, \tag{17}$$

with $R^2 = 0.9959$, $\Delta_{av} = 0.13\%$, and $\Delta_{max} = 1.12\%$ for Helium.

$$T_r^*\rho_{fr}^* = -0.2688\omega^2 + 0.5528\omega + 1.7317, \tag{18}$$

with $R^2 = 0.8388$, $\Delta_{av} = 0.60\%$, and $\Delta_{max} = 2.54\%$ for Methanol.

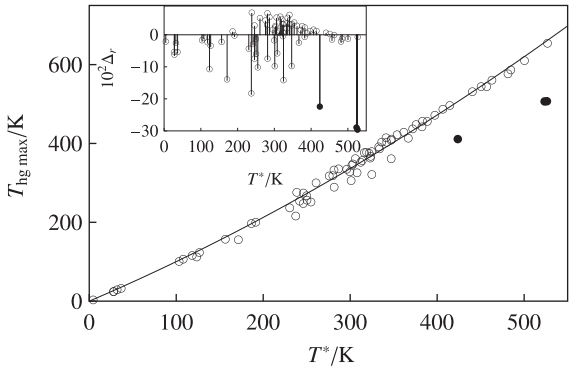

FIGURE 7. Plot of $T_{h_g\,max}$ *vs.* T^*. The symbols are the values obtained for the 75 fluids included in the NIST Chemistry WebBook [18] (see tables S1 and S2 of the supplementary data). H_2O, D_2O and Methanol are plotted with filled circles. The solid line represents the quadratic fit to the data given by equation (19). The inset shows the percent relative deviations of $T_{h_g\,max}$.

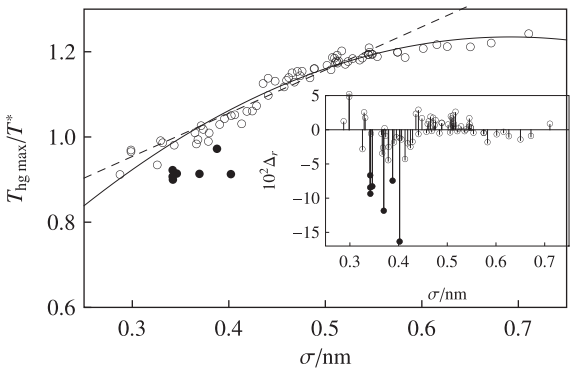

FIGURE 8. Plot of $T_{h_g\,max}/T^*$ *vs.* σ/nm. The symbols are the values obtained for the 75 fluids included in the NIST Chemistry WebBook [18]. The fluids that do not strictly follow the correlation are plotted with filled circles. The solid line represents a quadratic fit to the data [equation (20)] and the dashed line is the linear correlation proposed by Srinivasan [17]. The inset shows the percent relative deviations of $T_{h_g\,max}/T^*$.

TABLE 1
Comparison of predicted and tabulated values for two new low GWP refrigerants.

Property	HFO 1234yf [20–22]		HFO 1234ze [23,24]	
	Calculated	Tabulated	Calculated	Tabulated
T^*/K (1)	299	299	311	311
ρ_f^*/kg · m^{-3} (10)	1072	1089	1092	1119
T_{sp1}/K (12)	273.9	273.2	285	285
T_{sp2}/K (13)	324.7	325	337.9	339
p_{sp1}/MPa (14)	0.355	0.315	0.379	0.328
p_{sp2}/MPa (15)	1.379	1.366	1.480	1.500
ω (17)	0.241	0.280	0.248	0.296
$T_{h_g\,max}$/K (19)	335.3	349.5	350.8	362.5
σ/nm (9)	0.498	–	0.495	–

4. Third formulation: the maximum of the saturated vapor enthalpy curve

Srinivasan [17] finds that the saturated vapor enthalpy has a maximum at a particular temperature ($T_{h_g\,max}$) and the ratio of this temperature to T^* bears a linear relationship with the molecular diameter. Figure 7 shows that the relation between T^* and $T_{h_g\,max}$ is not exactly linear but can be correlated through a quadratic equation as given below:

$$T_{h_g\,max}/\mathrm{K} = 5.935 \times 10^{-4}(T^*/\mathrm{K})^2 + 0.9429(T^*/\mathrm{K}), \qquad (19)$$

with $R^2 = 0.9905$, $\Delta_{av} = 4.81\%$, and $\Delta_{max} = 29.88\%$ for H_2O. A few fluids that do not strictly follow the above generalized correlation are H_2O, D_2O and Methanol. This correlation also generally implies that $T_{h_g\,max} > T^*$.

However, the linear correlation between σ and $T_{h_g max}$ proposed by Srinivasan [17] fails to be satisfied when extended to the whole range of fluids as seen in figure 8. A correlation that best describes the data is

$$T_{h_g\,max}/T^* = -2.0282(\sigma/\mathrm{nm})^2 + 2.8175(\sigma/\mathrm{nm}) + 0.2577, \qquad (20)$$

with $R^2 = 0.9427$, $\Delta_{av} = 2.18\%$, and $\Delta_{max} = 16.46\%$ for Xenon. We note that Hydrogen, Parahydrogen, Helium, Argon, Krypton, Xenon and Methanol show a large deviation in figure 8 and have not been considered in the correlation.

The engineering implications of the above findings are as follows. Seldom practical thermodynamic cycles operate at temperatures higher than $T_{h_g\,max}$. An exception to this is the transcritical carbon dioxide ($T_{h_g max} = -24.5$ °C) refrigeration cycle when operating for medium temperature supermarket refrigeration or air conditioning. Between $T_{h_g\,max}$ and T_c the isentropes and the saturated vapor line diverge implying that a large desuperheating zone would be required for condensation of vapors. Ideally, one would like to have the compression isentropes to be close to the saturation curve in the superheated vapor region on the pressure-enthalpy plane, which happens for refrigerants such as propane. This is possible only when condensation temperatures are below $T_{h_g max}$. The flattening of the curve in figure 8 at high values of the molecular length parameter implies that $T_{h_g max} \to T_c$ and hence the critical region of the saturated vapor enthalpy curve has a plateau.

5. Predictions

One of the main goals of the correlations presented in this work is to demonstrate their usefulness for performing predictions of saturated properties of emerging refrigerants. As a check of the predictions given by the above correlations we have considered two new low GWP refrigerants HFO 1234yf and HFO 1234ze (E) for which recent results are available [20–24]. In the case of HFO 1234yf, $T_c = 367.85$ K, $p_c = 3.382$ MPa and $\rho_c = 477$ kg/m^3 [20–22] and for HFO 1234 ze(E), $T_c = 382.52$ K, $p_c = 3.632$ MPa and $\rho_c = 486$ kg/m^3 [23]. Our predictions for HFO 1234yf and HFO 1234ze (E) are presented in table 1 where we compare with data obtained from published results [20–24]. By and large the data corresponding to the maxima are in good agreement. However, there is a moderately large difference in the acentric factors, which is not surprising since the acentric factors are obtained from the correlation presented in equation (17), which itself requires data from the correlations given by equations (13) and (15). An alternative way of obtaining the acentric factors is via equation (16) that in turn requires data from equations (12) and (14). This alternative way yields even worse results because of the scatter in the data for p_{sp2}, as shown in figure 5.

6. Summary

To summarize, the occurrence of maxima in products of a few liquid–vapor saturation properties has been revisited and a few interesting linear empirical relations have been derived between the critical properties and properties at the temperatures of the maxima. More concretely, we have found that the temperature T^* where the $T\rho_f$ attains a maximum value shows a nice linear correlation with the critical temperature T_c, and also the molecular length parameter σ and the density ρ_f^* at this point are linearly related to their corresponding critical properties σ_c and ρ_c, respectively. Furthermore, the temperatures and pressures of the maxima of

$T_r(1-p_r)$ and $p_r(1-T_r)$ have been shown to present linear correlations with T_c and p_c. In addition, we have shown that the maximum values of the considered products are well correlated with the acentric factor. Finally, the temperature $T_{h_g\,max}$ where the saturated vapor enthalpy has a maximum has been shown to correlate well with T^* and the ratio of these two temperatures shows a quadratic correlation with σ. As a practical application of our results we have predicted the properties of two of the new low GWP refrigerants HFO 1234yf and HFO 1234ze (E) with good success.

Acknowledgements

S.V. and J.A.W. thank financial support by Ministerio de Educación y Ciencia of Spain under Grant FIS2009-07557. We would like to thank an anonymous reviewer for very useful comments on the manuscript.

Appendix A. Supplementary data

Tables S1 and S2 of the critical parameters and other quantities obtained from the 75 fluids available in the NIST Chemistry WebBook [18] can be found in the online version. Supplementary data associated with this article can be found, in the online version, at doi:10.1016/j.jct.2011.08.005.

References

[1] S. Khan, K. Srinivasan, High Temp. High Press. 26 (1994) 427–438.
[2] S. Khan, K. Srinivasan, High Temp. High Press. 26 (1994) 519–530.
[3] S. Khan, K. Srinivasan, J. Phys. D: Appl. Phys. 29 (1996) 3079–3088.
[4] K. Srinivasan, M.V. Krishna Murthy, Int. J. Refrig. 8 (1985) 143–146.
[5] K. Srinivasan, in: Proceedings of the Australian Bicentennial International Congress on Mechanical Engineering, volume 88/6, Institution of Engineers, Brisbane, Australia, 1988, pp. 79–83.
[6] P. Liley, Ind. Eng. Chem. Res. 42 (2003) 6250–6251.
[7] F.L. Roman, J.A. White, S. Velasco, A. Mulero, J. Chem. Phys. 123 (2005) 124512-1–124512-6.
[8] I. Cachadiña, A. Mulero, J. Phys. Chem. Ref. Data 36 (2007) 1133–1139.
[9] S. Velasco, F.L. Román, J.A. White, A. Mulero, Appl. Phys. Lett. 90 (2007) 141905-1–141905-3.
[10] K. Srinivasan, Chem. Eng. J. 81 (2001) 63–67.
[11] K. Srinivasan, Z. Phys. Chem. 216 (2002) 1379–1387.
[12] S. Velasco, J.A. White, J. Chem. Eng. Data 56 (2011) 1163–1166.
[13] K. Srinivasan, Acustica 74 (1989) 168–170.
[14] K. Srinivasan, M.V. Krishna Murthy, Int. J. Heat Mass Transfer 29 (1986) 1963–1967.
[15] S. Velasco, F.L. Romn, J.A. White, J. Chem. Eng. Data 55 (2010) 4244–4247.
[16] J. Tian, H. Jiang, Y. Xu, Mod. Phys. Lett. B 23 (2009) 3091–3096.
[17] K. Srinivasan, Chem. Phys. Lett. 179 (1991) 268–270.
[18] E. Lemmon, M. McLinden, D. Friend, NIST Chemistry WebBook, NIST Standard Reference Database Number 69, National Institute of Standards and Technology, Gaithersburg MD, 20899, 2011. <http://www.webbook.nist.gov> (retrieved 21.01.2011).
[19] B. Smit, J. Chem. Phys. 96 (1992) 8639–8640.
[20] M. Richter, M.O. McLinden, E.W. Lemmon, J. Chem. Eng. Data 56 (2011) 3254–3264.
[21] K. Tanaka, Y. Higashi, Int. J. Refrig. 33 (2010) 474–479.
[22] R. Akasaka, K. Tanaka, Y. Higashi, Int. J. Refrig. 33 (2010) 52–60.
[23] M.O. McLinden, M. Thol, E.W. Lemmon, in: International Refrigeration and Air Conditioning Conference at Purdue, July 12–15, 2010.
[24] K. Tanaka, G. Takahashi, Y. Higashi, J. Chem. Eng. Data 55 (2010) 2169–2172.